

---

# A COMPARATIVE ASSESSMENT OF DEEP LEARNING MODELS FOR DAY-AHEAD LOAD FORECASTING: INVESTIGATING KEY ACCURACY DRIVERS

---

**Sotiris Pelekis**

Decision Support Systems Laboratory School of Electrical and Computer Engineering  
National Technical University of Athens  
Athens, 15773  
spelekis@epu.ntua.gr

**Ioannis-Konstantinos Seisopoulos**

Decision Support Systems Laboratory School of Electrical and Computer Engineering  
National Technical University of Athens  
Athens, 15773  
giannisiso7@gmail.com

**Evangelos Spiliotis**

Forecasting and Strategy Unit School of Electrical and Computer Engineering  
National Technical University of Athens  
Athens, 15773  
spiliotis@fsu.gr

**Theodosios Pountridis**

Decision Support Systems Laboratory School of Electrical and Computer Engineering  
National Technical University of Athens  
Athens, 15773  
theopountridis@gmail.com

**Evangelos Karakolis**

Decision Support Systems Laboratory School of Electrical and Computer Engineering  
National Technical University of Athens  
Athens, 15773  
vkarakolis@epu.ntua.gr

**Spiros Mouzakit**

Decision Support Systems Laboratory School of Electrical and Computer Engineering  
National Technical University of Athens  
Athens, 15773  
smouzakit@epu.ntua.gr

**Dimitris Askounis**

Decision Support Systems Laboratory School of Electrical and Computer Engineering  
National Technical University of Athens  
Athens, 15773  
askous@epu.ntua.gr

February 24, 2023

**Nomenclature**

ANN	Artificial neural network
CNN	Convolutional neural network
DL	Deep learning
LSTM	Long short-term memory
LW	Lookback window
MAPE	Mean absolute percentage error
MLOps	Machine learning operations
MLP	Multi-layer perceptron
MLR	Multiple linear regression
N-BEATS	Neural basis expansion analysis time series forecasting
RMSE	Root mean squared error
RNN	Recurrent neural network
sNaive	Seasonal naive
STLF	Short-term load forecasting
TCN	Temporal convolutional network
TPE	Tree-structured parzen estimator

**ABSTRACT**

Short-term load forecasting (STLF) is vital for the daily operation of power grids. However, the non-linearity, non-stationarity, and randomness characterizing electricity demand time series renders STLF a challenging task. To that end, different forecasting methods have been proposed in the literature for day-ahead load forecasting, including a variety of deep learning models that are currently considered to achieve state-of-the-art performance. In order to compare the accuracy of such models, we focus on national net aggregated STLF and examine well-established autoregressive neural networks of indicative architectures, namely multi-layer perceptrons, N-BEATS, long short-term memory neural networks, and temporal convolutional networks, for the case of Portugal. To investigate the factors that affect the performance of each model and identify the most appropriate per case, we also conduct a post-hoc analysis, correlating forecast errors with key calendar and weather features. Our results indicate that N-BEATS consistently outperforms the rest of the examined deep learning models. Additionally, we find that external factors can significantly impact accuracy, affecting both the actual and relative performance of the models.

**Keywords** Short-Term Load Forecasting, Deep Learning, Ensemble, N-BEATS, Temporal Convolution, Forecasting Accuracy

**1 Introduction****1.1 Background**

Electricity load forecasting is crucial for the optimal operation and modernization of power systems (e.g. smart grids) and has always been an important task for all countries worldwide irrespective of their economical state. This is because power systems are the backbone of modern life, enabling all of the technology that organizations and individuals use to function within society. Load forecasts contribute in preserving the balance between electricity consumption and production, the economic power dispatch, storage scheduling, network planning, and expansion of power grids. However, electricity demand depends on numerous external variables [55], such as energy prices, weather conditions and demographics [46], as well as social and political factors like the climate crisis and the recent outbreak of the Russian-Ukrainian war that urge for an immediate energy transition through an even higher penetration of RES [57].

These factors complicate the patterns of load time series and therefore sophisticated models are required to accurately extrapolate them in time.

Load forecasting is typically divided into four categories according to the forecasting horizon considered. Long-term load forecasting involves forecasts up to 20 years ahead and is usually linked to grid development and strategic planning. Medium-term load forecasting involves a week up to a year ahead forecasts and is mainly used for maintenance scheduling and fuel purchases planning, as well as for energy trading and revenue assessment. Short-term load forecasting (STLF) includes one day to one week ahead forecasts. The resolution of said forecasts ranges from 15-minutes to one hour and they usually serve the day-to-day operations of utilities and companies participating in electricity markets. Lastly, very short-term load forecasting addresses forecast horizons of few minutes to few hours, being mostly used for demand response and near real-time control [17].

Focusing on STLF, it is considered a challenging task as electricity load time series are characterized by non-linearity, non-stationarity, noise, and multiple seasonal patterns. This can be attributed to the fact that electrical power demand originates from various electrical loads that, in turn, depend on numerous external variables, including weather and calendar factors. Additionally, the necessity for higher penetration of RES urges for more accurate forecasts that effectively adapt to the flexibility and demand response requirements posed within transmission and distribution operation systems. As a result, STLF has been investigated in a variety of research studies and projects [5, 44, 29, 42, 62].

## 1.2 Related work

Recently, artificial neural networks (ANNs) and deep learning (DL) models have dominated the field of time series forecasting including STLF among other energy forecasting applications. The multi-layer perceptron (MLP) architecture has been widely used for STLF [23, 27, 4], even though not originally designed to model time series data that are chronologically correlated. Other approaches that include genetic algorithms have also been proposed to reduce training time [32, 8] and to select the training parameters of genetic algorithm neural network hybrid models [61, 35]. ANNs have also been trained using artificial immune system models, mainly for hyperparameter tuning purposes [19, 12], and implemented in the form of extreme learning machines [67]. Moreover, several ensembling techniques have been introduced to reduce model and parameter uncertainty and, consequently, improve forecasting accuracy [61, 11]. An exhaustive review on ANN methods for STLF has been conducted by Hernandez et al. [20].

With respect to more recent advances, a massive flow of research studies have shifted towards deeper architectures [13]. Recurrent neural networks (RNN) and particularly long short-term memory (LSTM) neural networks [24] and their variants, such as sequence-to-sequence models and encoder-decoder architectures, cover a significant share of the current research interest on STLF [53, 51, 18]. Other innovative approaches build on convolutional neural networks [CNNs; 41] and LSTM hybrids since they can efficiently correlate load data with numerous weather variables [52, 47].

Cutting-edge DL architectures include temporal convolutional networks (TCN) [6], neural basis expansion coefficient analysis (N-BEATS) [39], and transformers [34]. These models have recently drawn considerable attention in the field of STLF as they can result to relatively higher accuracy, lower training times, and more interpretable forecasts [33, 39]. Specifically, Tang et al. [59] employed a TCN architecture with channel and temporal attention mechanisms to exploit the non-linear relationships between weather factors and load. Yin and Xie [65] applied a multi-temporal-spatial-scale TCN for forecasting the load of a city in China, while Gu and Jia [15] compared the TCN architecture with three traditional models, suggesting its superiority when used to forecast the load of a certain region in Shanghai. Regarding N-BEATS, it has been evaluated by Oreshkin et al. [40] on medium-term load forecasting tasks, achieving state-of-the-art performance, and by Singh et al. [54], who employed the model for STLF in Ontario. Wen et al. [63] and Grabner et al. [14] have also used variants of N-BEATS for probabilistic STLF and consumer-level STLF at global scale, respectively. In addition, Pelekis et al. [44] compared the accuracy of TCN and N-BEATS in STLF settings for the case of the Portuguese national load at a 15-minute resolution, with N-BEATS resulting to superior forecasts. With respect to transformers, Zhang et al. [66] evaluated a time augmented transformer for STLF on the electrical load data of New South Wales in Australia, Lim et al. [33] validated temporal fusion transformers for STLF on the UCI Electricity Load Diagrams Dataset [60], while Huy et al. [25] employed the latter architecture to forecast the load of Hanoi city using weather and calendar features.

Another research topic of great interest and implications in time series forecasting is the explainability of forecasting performance. Spiliotis et al. [56] investigated the time series features of popular forecasting competition data sets, concluding that different forecasting methods should be used depending on the particularities of the data. Their analysis built on established feature extraction and visualization techniques [28], as well as a multiple linear regression (MLR) model that correlated time series feature values with forecasting accuracy. This type of explanatory analysis was first introduced by Petropoulos et al. [45], proposing the selection and combination of different forecasting models based on their expected forecast accuracy, predicted based on key time series features. In a similar direction, Montero-Manso

et al. [37] used a tree-based model to combine the forecasts of various models based on time series features, while Talagala et al. [58] introduced a meta-learning algorithm for time series forecast model performance prediction and selection, also providing useful insights on which forecasting models best work for particular types of time series. In the STLF domain, Moon et al. [38] proposed an explainable tree-based model to forecast the demand in buildings using Shapley values [50], concluding that the temperature-humidity index and the wind chill indexes affect the forecasting accuracy more than temperature, humidity, and wind speed. Similarly, Wu et al. [64] used Shapley values to develop a feature selection strategy for load forecasting models within a regional integrated energy system.

### 1.3 Contribution

In this study, a comparative assessment of state-of-the-art DL architectures is performed and the impact of key external factors (calendar and weather features) on their forecasting accuracy is investigated. Our analysis focuses on day-ahead forecasts and net aggregated load time series, using the Portuguese electricity transmission system as a representative case-study. The main contributions of the study are summarized as follows:

- (a) We consider four well-established autoregressive DL models and evaluate their accuracy for 24-hour-ahead forecasts. This includes the MLP, N-BEATS, TCN, and LSTM architectures that have recently drawn significant attention in the field of STLF. To enhance the representativeness of our results, we carefully tune the hyperparameter values of the models and produce forecasts for a complete calendar year using ensembles. Moreover, we benchmark the performance of the DL models using standard baseline models.
- (b) We use MLR to correlate calendar (time of day, season, holidays, and weekends) and weather (temperature) features with the forecast errors of each DL model. Effectively, this post-hoc analysis enables us to decompose the forecasting performance of the examined models and identify the factors that deteriorate their accuracy most. Moreover, it allows us to identify models that are expected to perform best based on the calendar and weather features of the period being forecast. As a result, this analysis provides valuable insights to energy stakeholders interested in reinforcing their forecasting toolkits with state-of-the-art DL techniques or producing forecasts in a selective fashion.
- (c) In addition to the above, we expand the analysis conducted by Pelekis et al. [44] in three dimensions. First, we focus on purely autoregressive models, thus assessing the performance of DL time series forecasting models that do not require weather forecasts or any other type of external information as additional input. Second, we utilize high performance computing infrastructures to properly tune the examined models and evaluate their performance when used individually or within ensembles. By doing that, we investigate the robustness of each neural network architecture to random neural weight initializations and confirm the benefits of combining. Third, our analysis is performed on a newer version of the data set (ranging from 2013 to 2021 instead of 2019) that has a resolution of one hour instead of fifteen minutes.

### 1.4 Structure of the paper

The rest of the paper is organized as follows. Section 2 describes our methodological approach, including the utilized DL architectures and benchmarks, the data used for the empirical evaluation, and the MLR framework employed to explain the forecasting performance of each model. Section 3 presents our results, while section 4 wraps up the paper, presenting concluding remarks and future perspectives.

## 2 Methodology

This section presents the methodology used to address the common stages of the machine learning life-cycle referring to our specific STLF case in Portugal. These stages include the following tasks: (i) data collection, wrangling and transformations; (ii) exploratory analysis of the data set; (iii) selection and description of utilized DL architectures; (iv) training and model validation (hyperparameter tuning); (v) forecast evaluation. Subsequently, the MLR-based framework used for explaining the forecasting performance of the DL models is presented. The experimental process took place using an automated machine learning operations (MLOps) pipeline developed with MLflow [2], building up to the one described by Pelekis et al. [44].

### 2.1 Data collection and exploratory analysis

The data set used in the present study consists of the time series of the Portuguese national net aggregated electricity demand, reported at an hourly time resolution. The data was acquired by the Portuguese transmission system operator Redes Energéticas Nacionais [49] that provides the data set online [48]. The time series ranges from 2013 to 2021 as

this was the most recent version of the data set including complete calendar years at the time the experiments were conducted. The operations applied to the electricity load time series before data scaling and model training took place were the following: (i) removal of duplicate entries (mainly caused by changes between standard and daylight saving time) and (ii) filling of missing data (rare cases handled using linear interpolation). An additional data source used was the the Copernicus [9] Climate Data Store [3] and precisely the "ERA5 hourly data on single levels from 1959 to present" data set [21]. This data set was utilized to extract air temperature measurements<sup>1</sup> at 2 meters above the surface of land, sea, or inland waters in the city of Lisbon. The temperature is calculated by interpolating between the lowest model level and the Earth's surface, taking into account the atmospheric conditions.

Autoregressive models can be used to predict the future values of a time series by looking back at a predefined number of its past values. However, as already discussed, various exogenous variables can affect electricity demand, thus influencing the performance of forecasting models. To demonstrate this effect, we analyze the daily load profiles of the time series in juxtaposition to these exogenous factors. Figure 1 demonstrates the variation of daily load profiles given certain calendar features. Specifically, Figure 1a illustrates the average daily load of Portugal as a reference point, while Figures 1b, 1c, and 1d present the average daily load on holidays versus non-holiday days, weekends versus weekdays, and the inter-season daily profiles respectively. We observe that on holidays a) the lower load values during the early morning hours are shifted towards later hours of the day as citizens tend to wake up later; b) load exhibits a lower mean value than non-holiday days; c) a notable load decrease during working hours; d) a peak shift towards later hours regarding the usual night peak of 8 p.m. Similar conclusions can be drawn for weekends and weekdays with the exception of the late night peak shift. Regarding the per season average load profiles, the deviations among seasons is still visible with the naked eye. However, during the winter period, a wider downward peak can be noticed during the morning hours alongside a notably faster load decrease during the late afternoon hours. These juxtapositions clearly reveal the variation of load according to the examined calendar features and hence reveal a certain correlation that, in turn, encourages model selection based on these factors.

Regarding the intra-day fluctuations, from the average daily profile of Figure 1, four main intervals of varying time series behavior can be observed:

- **early morning** (23.00-04.00): During these hours an almost linear and decreasing pattern can be observed in the load profile given that most companies do not operate and households gradually reduce their electrical energy consumption.
- **morning** (04.00-09.00): A steadily increasing trend is observed within the load profile curve as every day life gradually recovers to its usual patterns;
- **midday** (09.00-17.00): This is a volatile period of the day corresponding to ordinary working hours. The load curve is noisy, however it maintains a rather constant level within this interval.
- **night** (17.00-23.00): A convex curve can be observed, corresponding to the consumption of peak hours, followed by the late night drop caused by the termination of most daily activities.

These intra-day patterns could also imply potential drifts of forecasting performance across different models, hence further supporting conditional model selection.

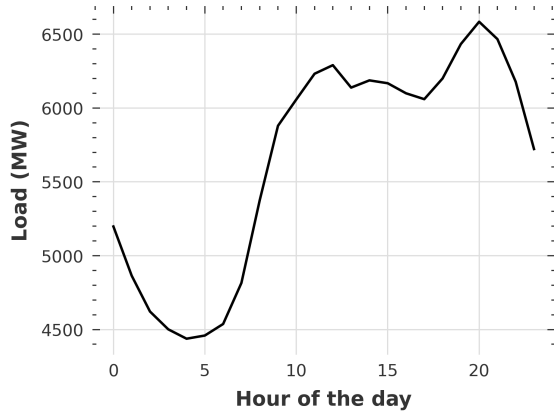
## 2.2 Selected models and benchmarks

To conduct our comparative analysis, a targeted model selection procedure took place aiming to demonstrate the differing aspects of current state-of-the-art DL architectures. When evaluating forecasting models, it is necessary to introduce concrete benchmarks and, in this direction, two seasonal naive (sNaive) models of daily and weekly seasonality were employed. Additionally, to investigate the value added by more sophisticated and deeper architectures compared to traditional ANNs, a MLP model was also developed. LSTM networks have been considered as standard choices for STLF, while N-BEATS and TCN have been more recently introduced, thus serving as representative DL architectures. The selected DL models and benchmarks are presented below in more detail:

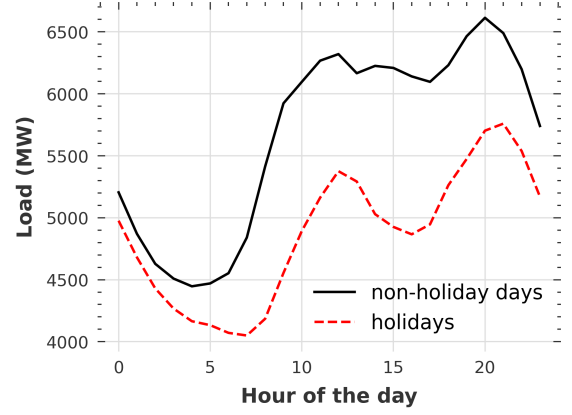
**sNaive (24)** This naive model of daily seasonality uses the observed values of the previous day as day-ahead forecasts. The method is expected to generate poor results as electricity load time series exhibit multiple seasonal cycles, being strong at both daily and weekly level.

---

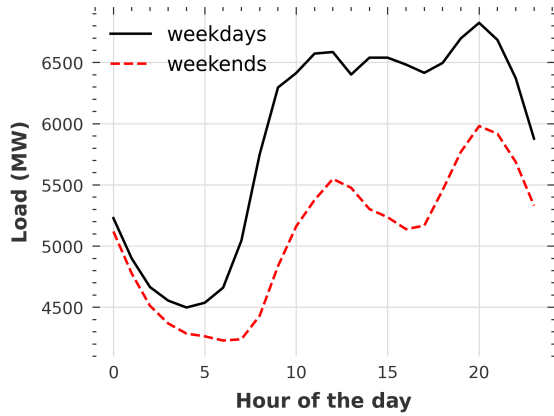
<sup>1</sup>As explained, temperature and calendar features will be used in the post-hoc analysis of the study to explain the forecasting performance of the examined DL models.



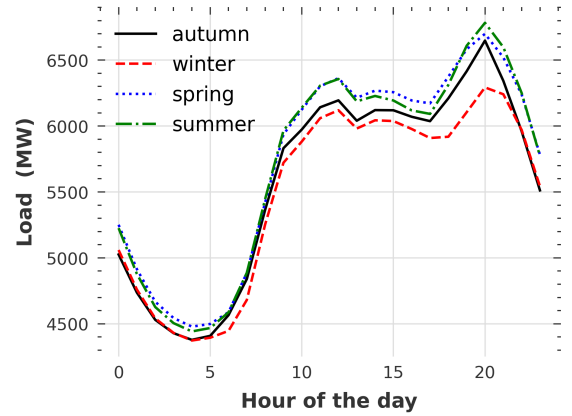
(a) Average daily electricity load over the complete data set.



(b) Average daily electricity load across holidays and non-holiday days.



(c) Average daily electricity load across weekends and weekdays.



(d) Average daily profiles across different seasons of the year.

Figure 1: Average daily profiles of the Portuguese national electricity load time series grouped by selected calendar features relating to seasons, time of day, holidays, and weekends.

**sNaive (168)** This naive model of weekly seasonality uses the observed values of the same day of the previous week as day-ahead forecasts. The method is expected to produce moderate results as it can effectively take into account daily and weekly seasonality.

**Multi-layer perceptron (MLP)** This is the most common DL architecture, consisting of multiple perceptrons (or neurons) arranged in multiple layers. Each individual neuron's output is calculated using the function of Equation 1.

$$y = f\left(\sum_{i=1}^n (w_i x_i) + b\right) \quad (1)$$

The weighted (with weights  $w_i$ ) sum of the outputs ( $x_i$ ) of all the neurons in the previous layer plus a bias term ( $b$ ) is computed first. Then, the activation function  $f$  is applied to this result. The purpose of this function is to enable the model to capture nonlinear relationships among the inputs (lags) and outputs (forecasts). Various activation functions have been used in literature, the most popular being the rectified linear unit (ReLU) of Equation 2.

$$f(x) = \frac{1}{1 + e^{-x}} \quad (2)$$

During the training process of a MLP, the backpropagation algorithm is used. The weights and biases of the MLP are iteratively updated according to the following equation

$$w_{ij}^k(t+1) = w_{ij}^k(t) - \alpha \frac{\partial L}{\partial w_{ij}^k}, \quad (3)$$

where  $w_{ij}^k(t)$  is the weight connecting the  $i$ -th neuron of a layer with the  $j$ -th neuron of the previous layer at iteration  $t$  of the algorithm,  $\alpha$  is the learning rate, and  $L$  is the loss function. The gradient is computed using the chain rule, and the algorithm needs to be run after each forward pass of the training.

In this study, the Scikit-Learn [43] machine learning toolkit was used for implementing the MLP model.

**Long short-term memory (LSTM)** LSTM is an extension of the classical RNN that came to solve the vanishing gradient problem, mitigating RNNs' inability to learn long range dependencies [24]. LSTM has been extensively used for sequence modeling and time series forecasting. It is capable of learning long-term dependencies by introducing a memory cell and three different gates, namely the input gate, output gate, and forget gate. This allows the network to store information over a large number of time steps, which is crucial for time series forecasting. The LSTM architecture can be represented mathematically as shown below:

$$\begin{aligned} f_t &= \sigma(W_f \cdot [h_{t-1}, x_t] + b_f), \\ i_t &= \sigma(W_i \cdot [h_{t-1}, x_t] + b_i), \\ o_t &= \sigma(W_o \cdot [h_{t-1}, x_t] + b_o), \\ g_t &= \tanh(W_g \cdot [h_{t-1}, x_t] + b_g), \\ c_t &= f_t \cdot c_{t-1} + i_t \cdot g_t, \\ h_t &= o_t \cdot \tanh(c_t), \end{aligned} \quad (4)$$

where  $f_t, i_t, o_t$  are the forget, input, and output gates,  $g_t$  is the cell state,  $c_t$  is the memory cell,  $h_t$  is the hidden state at time step  $t$ , and  $b_k$  the respective bias of gate  $k$ . Backpropagation through time is used to train calculate the gradients of LSTM architecture and gradually update their weights.

Focusing on encoder-decoder architectures, they can be used for time series forecasting by recurrently encoding the input sequence into a fixed length vector, and then recurrently decoding it back into a sequence of predictions as the encoder and decoder are typically implemented using RNNs and more often LSTMs. The hidden dimension of the encoder and decoder is an important hyperparameter that needs to be the same for the two components in order for the model to function properly. Another important hyperparameter of an encoder-decoder LSTM is the number of recurrent layers in the encoder and decoder. Typically, increasing said number leads to more complex models that are prone to overfitting and generalize poorly on previously unseen data. Hence, the selection of these hyperparameters should be handled with care. The encoder-decoder architecture can be represented as shown below:

$$\begin{aligned} h_t &= \text{LSTM}_{\text{encoder}}(x_t) \\ \hat{y}_t &= \text{LSTM}_{\text{decoder}}(h_t) \end{aligned} \quad (5)$$

where  $h_t$  is the hidden state of the encoder at time step  $t$  and  $\hat{y}_t$  is the forecast at the same step.

In this study, the Darts [22] forecasting toolkit was used for implementing the LSTM model, exploiting the BlockRNN-Model class.

**Neural basis expansion analysis time series forecasting (N-BEATS)** N-BEATS is a deep feed-forward neural network, introduced by Oreshkin et al. [39] in an attempt to demonstrate that a pure autoregressive DL models can outperform traditional forecasting methods. The N-BEATS architecture consists of  $n$  stacks, which comprise  $m$  fully connected non-linear neural regressor blocks, interconnected with double residual links. Each block has a fully connected stack of  $k$  layers using the ReLU activation function. The first block receives an input  $\hat{x}_1 \equiv \hat{x}$ , whereas the other blocks receive an input  $\hat{x}_m$ , producing two distinct outputs, namely the backcast  $\hat{b}_m$  and the forecast  $\hat{f}_m$ . The former ( $\hat{b}_m$ ) is subtracted from the input of the next block as in Equation 6 and is referred to the part of the input that has been predicted adequately, while the latter ( $\hat{f}_m$ ) is a partial forecast to predict the future.

$$\hat{x}_m = \hat{x}_{m-1} - \hat{b}_{m-1} \quad (6)$$

This strategy is called double residual stacking and contributes to both forecasting and decomposing the target time series. The outputs of the blocks ( $\hat{f}_m$ ) are aggregated to produce the forecast ( $\hat{f}_n$ ) of each stack, as shown in Equation 7, and it is used to calculate the loss function and train the model.

$$\hat{f}_n = \sum_{i=1}^m \hat{f}_m \quad (7)$$

Finally, the outputs ( $\hat{f}_n$ ) of the stacks are combined to produce the forecast ( $\hat{y}$ ) of the model, as shown in Equation 8.

$$\hat{y} = \sum_{i=1}^n \hat{f}_n \quad (8)$$

In this study, the Darts forecasting toolkit was used for implementing the N-BEATS model. The generic form of the architecture was used without considering the ensembles originally proposed by Oreshkin et al. [39].

**Temporal convolutional network (TCN)** TCN, first introduced by Bai et al. [6], is a type of neural network architecture that has been specifically designed for processing sequential data. Specifically, TCN is a CNN that consists of dilated, causal 1-dimensional convolutional layers with the same input and output lengths. Stack dilated convolutional networks are constructed to capture long term temporal dependencies, enabling large receptive fields with the use of a reasonable amount of layers. Equation 9 shows the basic formula characterizing a temporal convolutional layer

$$y[i] = b[i] + \sum_j w[i, j] * x[j], \quad (9)$$

where  $x$  is the input sequence,  $w$  is the weight matrix of the layer,  $b$  is the bias vector,  $y$  is the output sequence, while  $i$  and  $j$  are the indexes of the time step in the input and output sequence, respectively. The depth of the network is determined by the number of convolutional layers while the width of the network is determined by the number of filters in each convolutional layer. The size of the kernel plays a crucial role, allowing the network to learn more global patterns in the data. The residual block has a doublet of dilated convolutional layers followed by a batch normalization operation and a ReLU activation. Regarding the receptive field ( $R$ ) of a TCN, it is usually calculated using the number of convolutional layers ( $l$ ), the dilation base ( $b$ ), and the kernel size ( $k$ ), as shown in Equation 10. The purpose of such calculation is to assure that the receptive field is large enough to process the input variables.

$$R = b^l \cdot (k - 1) \quad (10)$$

In this study, the Darts forecasting toolkit was used for implementing the TCN model.

### 2.3 Model Training

The objective of the training process has been the development of DL models for day-ahead load forecasting at hourly resolution for the net aggregated electricity demand of the Portuguese transmission system. In this context, the selected DL architectures were trained on multiple sets of hyperparameter values using the tree-structured parzen estimator (TPE) hyperparameter optimization method, as described by Bergstra et al. [7] and implemented in Python programming language in Optuna optimization library [1].

Early stopping was applied with a patience of 10 epochs. A crucial hyperparameter that is common among all architectures, is the look-back window (LW), namely the number of historical time series values (lags) that the model looks back at when being trained to produce forecasts. Note that LW directly determines the input layer size of the trained neural network. The specific details of the optimization process for each architecture are presented in Table 1 where only the hyperparameters that were tuned are presented, while the rest of the hyperparameters were set to their default values, as proposed by the respective Python implementation frameworks. A total of 100 trials were executed for the optimization each DL architecture. All models have been optimized to minimize the L2 loss, namely squared error loss, following a mini batch gradient computation approach.

Following the identification of the best model architecture in terms of hyperparameter values, 30 separate networks sharing the same hyperparameter values but different pseudo-random initializations of neural weights were trained for each DL architecture. Then, an ensemble of these models was used to produce the final forecasts. To improve the robustness of the results, the median operator was used to aggregate the forecasts of the individual models [31].



Table 1: The hyperparameters optimized per DL architecture and the respective search spaces.

Architecture	Hyperparameters	
	Name	Space
MLP	LW	{24, 48, ..., 480}
	layers	{1, 2, ..., 10}
	neurons / layer	{50, 60, ..., 200}
	activation	{relu, sigmoid}
	batch size	{256, 512, ..., 2048}
LSTM	LW	{24, 48, ..., 480}
	RNN layers	{1, 2, ..., 10}
	hidden dimension	{24, 48, ..., 240}
	batch size	{256, 512, ..., 2048}
N-BEATS	LW	{24, 48, ..., 480}
	stacks	{1, 2, ..., 25}
	blocks	{1, 2, ..., 20}
	layers	{1, 2, ..., 10}
	batch size	{256, 512, ..., 2048}
TCN	LW	{24, 48, ..., 480}
	kernel size	{2, 3, ..., 6}
	filters	{2, 3, ..., 12}
	dilation base	{2, 4, 8, 16, 32}
	batch size	{256, 512, ..., 2048}

Every DL model was: (i) trained on the train set (years 2013 to 2019: 61,344 data points); (ii) optimized on the validation set (year 2020: 8,784 data points) to identify appropriate hyperparameter values; (iii) and evaluated on the remaining, previously unseen test set (year 2021: 8,760 data points) without retraining the model on the full dataset. This split allowed the inclusion of complete calendar years within each set of data, thus maintaining the symmetry of seasonal patterns. Regarding the sampling procedure, the training set comprises  $N_{train}$  samples as shown in Equation 11.

$$N_{train} = k_{train} - LW - FH + 1 = 61,321 - LW \quad (11)$$

where  $k_{train}$  is the number of data points in the train set,  $FH$  the forecast horizon (24 hours), and  $LW$  the lookback window used by the model. Similarly, the validation set consists of  $N_{val}$  samples, as shown in Equation 12.

$$N_{val} = k_{val} - FH + 1 = 8,761 \quad (12)$$

where  $k_{val}$  is the number of validation data points. With respect to the testing process, the test set contains  $N_{test}$  samples, as shown in Equation 13, given that the model evaluation took place at a daily basis rather than hourly, considering daily forecast batches of 24 hours.

$$N_{test} = \frac{k_{test}}{FH} = 365 \quad (13)$$

All models have been trained on the scaled version of the time series using a normalization approach within the  $[0,1]$  space. Note here that scaling took place using the train set range of values. The training and validation of the models was executed on an Ubuntu 22.04 virtual machine with an NVIDIA Tesla V100 GPU, 32 CPU cores, and 64GB of RAM.

## 2.4 Evaluation of forecasting accuracy

With respect to the evaluation of forecasting accuracy, various forecasting performance measures are common in the literature, such as the mean absolute error (MAE), the mean squared error (MSE), the mean absolute percentage error (MAPE), the root mean square error (RMSE), the symmetric mean absolute percentage error (sMAPE), and the mean absolute scaled error (MASE) Hyndman and Koehler [26]. Within the present study, MAPE was used as it is a widely accepted choice in STLF applications and results to interpretable measurements. As a result, MAPE served as the

objective function during the hyperparameter optimization process and as the main evaluation measure. MAPE is defined as shown in Equation 14.

$$MAPE = \frac{1}{m} \sum_{i=1}^m \left| \frac{Y_t - F_t}{Y_t} \right| \cdot 100(\%) \quad (14)$$

where  $m$  represents the number of samples, while  $Y_t$  and  $F_t$  stand for the actual values and the forecasts at time  $t$ , respectively.

## 2.5 Multiple linear regression for forecasting performance explanation

Although forecasting accuracy measures like MAPE are useful for identifying models that perform best on average, they provide no information about the conditions under which the forecast accuracy of each model is typically improved or deteriorated. In order to provide intuitive insights in this direction, for each architecture, a MLR model was estimated to correlate the MAPE values of the test set (dependent variable) with nine key forecast accuracy drivers (independent variables), as follows:

- Three binary (one-hot encoded) features (F1: morning, F2: midday, F3: night), representing the **time of day**. The “early morning” variable was dropped from the model to avoid undesirable multicollinearity effects.
- Three binary features (F4: winter, F5: spring, F6: autumn), representing the **season of the year**. The “summer” variable was dropped to avoid undesirable multicollinearity effects.
- One binary feature (F7: holiday), representing the **Portuguese national holidays**. The “non-holiday” variable was dropped to avoid undesirable multicollinearity effects.
- One binary feature (F8: weekend), representing **weekends**. The “weekday” variable was dropped to avoid undesirable multicollinearity effects.
- One numerical feature (F9: temperature) representing the **temperature** in the city of Lisbon. This variable was introduced as an extra dependent variable in the MLR problem, as it is known to affect electricity load patterns [36, 10, 16].

Hence, each of the MLR models can be formulated as follows:

$$MAPE_k = aF1_k + bF2_k + \dots + hF3_k + iF9_k \quad (15)$$

where  $MAPE_k$  is the error generated for the  $k_{th}$  data point of the selected test set (year 2021) and  $F^i_k$  the value of variable  $F^i$  at the same point. Before estimating the models, both dependent (MAPE) and independent (external features) variables were 1% trimmed in order to mitigate the effect of extreme values and enhance the representativeness of the results.

Note that positive MLR coefficients suggest factors that have a negative impact on accuracy, while negative ones suggest factors that result to lower forecast errors. Also, each MLR model can effectively serve as a framework for decomposing forecasting performance, predicting forecast accuracy and, consequently, conditionally selecting the most appropriate forecasting model.

## 3 Results

In this section, the results of the study are presented and discussed, addressing two main aspects as follows:

- The macroscopic comparison and ranking of the selected DL architectures in terms of forecasting accuracy in the examined STLF task (Section 3.1).
- The detailed results of the MLR models, accompanied by explanatory comments regarding each architecture’s performance, as well as model selection insights based on the selected calendar and weather features (Section 3.2).

### 3.1 Forecasting accuracy

Initially, the results of the training and hyperparameter tuning processes are summarized, leading to the final architectures and weights for each of the selected forecasting methods. The computational times for running the 100 TPE trials are

Table 2: Evaluation of the selected DL methods on the test set (2021) in terms of forecasting accuracy (MAPE) and computational cost (minutes). The first column lists the average MAPE and standard deviation of the 30 models involved in each ensemble. The second column lists the performances of the respective ensemble models (median of individual forecasts). The third column reports the time required for tuning the hyperparameters of each architecture and training the models included in the ensembles.

Architecture	Accuracy (MAPE %)		Cost (minutes)
	Individual models	Ensemble	Tuning & training
sNaive (24)	6.51	-	1
sNaive (168)	4.29	-	1
MLP	$2.59 \pm 0.07$	2.34	253
LSTM	$2.63 \pm 0.14$	2.23	2,343
N-BEATS	$2.43 \pm 0.13$	1.90	2,983
TCN	$2.52 \pm 0.09$	2.22	5,349

also listed along with the times required for training the models of each ensemble as they are indicative of the resources needed in real life for their implementation. The results are as follows:

- **sNaive (24):** No optimization took place as there are no hyperparameters to tune. The method required 1 minute to produce forecasts for the complete test set.
- **sNaive (168):** No optimization took place as there are no hyperparameters to tune. The method required 1 minute to produce forecasts for the complete test set.
- **MLP:** The TPE optimization process of the MLP architecture ran for 191 minutes to converge to the following hyperparameter values: LW: 192, layers: 2, neurons per layer: [150, 160], activation function: relu, batch size: 512. Given these values, each model of the ensemble was trained for 2.03 minutes, using a total of 178 epochs. The method required 1 minutes to produce forecasts for the complete test set.
- **LSTM:** The TPE optimization process of the LSTM architecture took 1,664 minutes to converge to the following hyperparameter values: LW: 240, RNN layers: 3, hidden dimension: 48, batch size: 1,280. Given these values, each model of the ensemble was trained for 22.6 minutes, using a total of 180 epochs. The method required 1 minutes to produce forecasts for the complete test set.
- **N-BEATS:** The TPE optimization process of the N-BEATS architecture took 2589 minutes and resulted to the following set of hyperparameter values: LW: 192, stacks: 3, blocks: 6, layers: 3, batch size: 1,536. Note here that the layer widths and the dimension of the expansion coefficient have been set to 64 and 5 respectively. Given these values, each model of the ensemble was trained for 13.1 minutes, using a total of 108 epochs. The method required 1 minutes to produce forecasts for the complete test set.
- **TCN:** The TPE optimization process of the TCN architecture took 3,698 minutes to converge to the following set of hyperparameter values: LW: 456, kernel size: 4, filters: 10, dilation base: 8, batch size: 256. Given these values, each model of the ensemble was trained for 55 minutes, using a total of 296 epochs. The method required 1 minutes to produce forecasts for the complete test set.

Taking into consideration the ensembling modeling approach (median of 30 networks) that followed the hyperparameter optimization process, the final performance of each architecture for year 2021 is summarized in Table 2. Regarding the benchmarks, sNaive (128) performs much better than sNaive (24) as it replicates weekly seasonality which is significantly stronger in electricity load time series. Regarding the DL methods, the N-BEATS architecture clearly outperforms the respective MLP, LSTM, and TCN models in terms of forecasting accuracy, reaching a MAPE value of just 1.90%. TCN and LSTM perform similarly, but the former is computationally more expensive, both compared to LSTM and N-BEATS. The MLP follows with a competitive performance for an architecture that is much faster to run and not originally designed for handling sequential data, like time series. Additionally, we observe that all DL architectures outperform the sNaive benchmarks. This is an expected result as sNaive models simply replicate past values and do not involve any learning process. Last but not least, it is noticeable that although the validation set mainly contained a period that has been highly affected by the COVID-19 pandemic [44], the selected DL architectures manage to perform impressively well.

To validate the added value of the ensembling strategy, Table 2 lists both the average forecast error of the individual models involved in each ensemble and the respective standard deviation of said errors. These results are also visualized in Figure 2. As seen, the accuracy of the ensembles is always higher than that of the individual models, suggesting that the examined strategy cannot only ensure robustness by avoiding inaccurate forecasts, but also lead to superior accuracy overall.

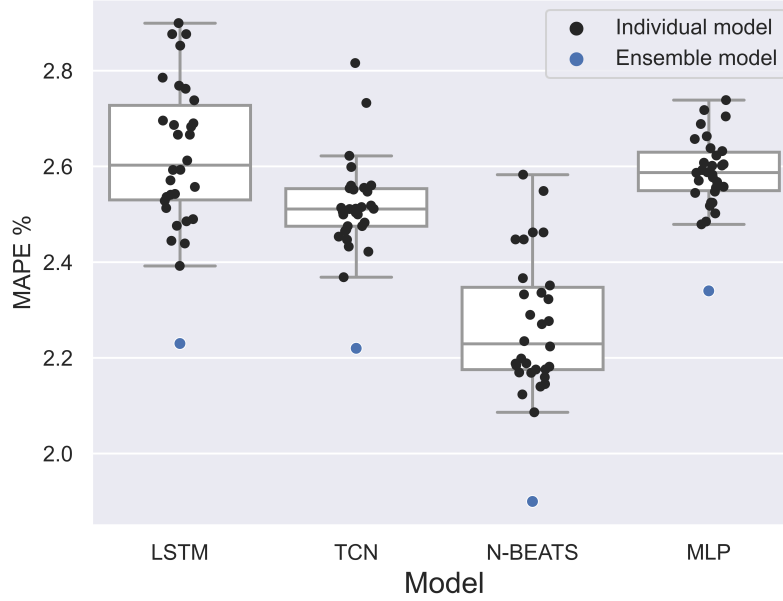


Figure 2: Boxplots summarizing the accuracy (MAPE) of the 30 individual models (same hyperparameter values but different neural weight initializations) used to form the ensemble of each DL architecture. The MAPE of the ensemble is also depicted.

To further investigate the differences reported between the examined DL methods and the benchmarks considered, we conduct the multiple comparisons with the best (MCB) test [30]. The test computes the average ranks of the forecasting methods according to MAPE across the complete test set and concludes whether or not these are statistically different. Figure 3 presents the results of the analysis. If the intervals of two methods do not overlap, this indicates a statistically different performance. Thus, methods that do not overlap with the gray interval of the figure are considered significantly worse than the best, and vice-versa. The results of the MCB test confirm that N-BEATS is significantly more accurate than the rest of the methods. TCN and LSTM are similarly accurate compared to each other, while MLP follows closely, being however significantly worse than the rest of the DL models. It is also clear that both benchmarks are significantly worse than any of the DL methods considered.

### 3.2 Explaining forecasting performance

Table 3 presents the coefficients estimated by the MLR models, aiming to explain the forecasting performance achieved by the DL methods and the benchmarks using as accuracy drivers the selected calendar and weather features. The goodness-of-fit coefficient  $R^2$  is also reported to measure the capability of the MLR models to identify strong correlations. Before interpreting the results of Table 3, the following should be noted:

- The calendar variables are binary and therefore their coefficients denote the extent to which the forecast error is increased on average during the time period they represent. On the contrary, temperature is a continuous variable, and the respective coefficients demonstrate the average increase in MAPE that is expected given a rise in the temperature by  $1^\circ C$ .
- The coefficients calculated by fitting the MLR models do not directly reflect the absolute fluctuations of the MAPE values across different models but rather the relative variation around the corresponding average value of a given model. This is rational as each MLR model is built independently for each forecasting method. As a result, the complementary bar charts of Figure 4 are required to establish a complete comparison among the different models in terms of accuracy. Appendix A also contains the bar charts that summarize forecasting accuracy according to the RMSE measure instead of MAPE. However, since the graphs of the two measures are very similar, the latter set of graphs is not discussed separately and included just for the sake of completeness.
- Drawing conclusions for the "early morning" hours and the "summer" periods is not possible due to the exclusion of these features from the MLR models to avoid severe multicollinearity problems. However, the selection of these variables was not random as these periods were usually characterized by lower forecast errors, thus exhibiting less interest for explanatory insights.

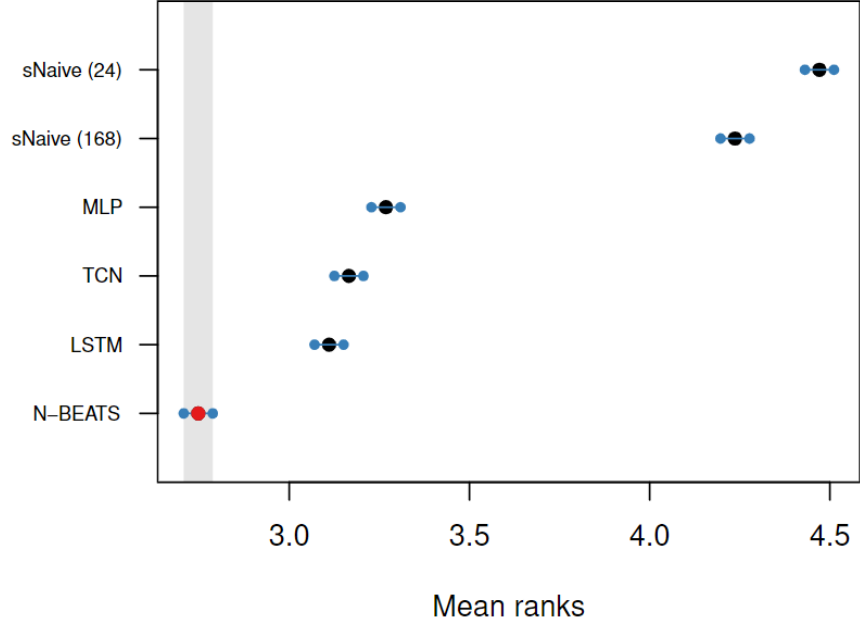


Figure 3: Average ranks and 95% confidence intervals of the four DL forecasting models and the two benchmarks considered in the present study. The multiple comparisons with the best test, as proposed by Koning et al. [30], is applied using MAPE for ranking the methods.

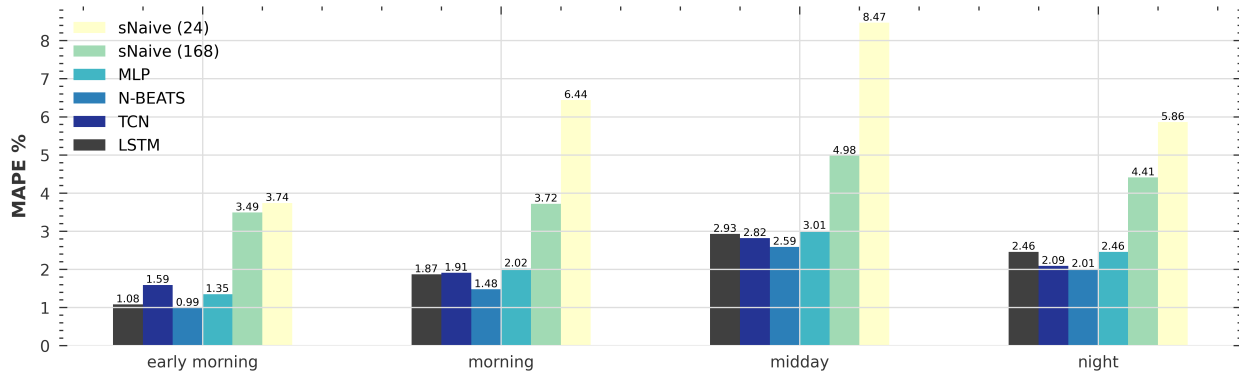
- The considered features explain more than half of the MAPE variance ( $R^2$  values higher than 0.5). Although including more external variables could result to higher  $R^2$  values, given the randomness of the series and the challenges present in STLF, we suggest that this value still suggests an adequate amount of explainability.
- All coefficients of the MLR model have proved to be statistically significant with p-values lower than 0.05. This reinforces the validity of the observations and conclusions extracted in the paragraphs to follow.

Table 3: Coefficients of the MLR models computed to relate the MAPE values generated by sNaive (24), sNaive (168), MLP, LSTM, N-BEATS, and TCN in the test set of the study with the selected calendar and weather features.

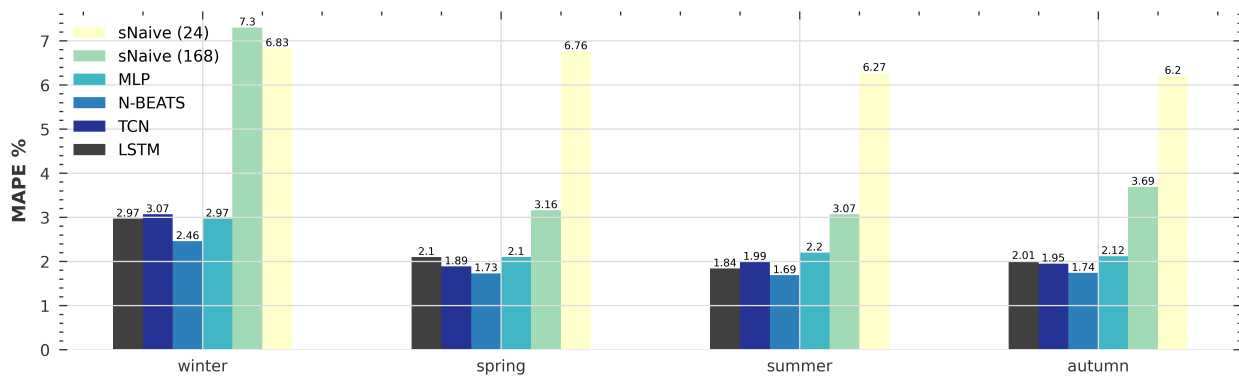
	morning	midday	night	winter	spring	autumn	holiday	weekend	temperature	$R^2$
<b>sNaive (24)</b>	2.89	4.61	2.18	1.21	0.87	0.29	4.91	6.01	0.07	0.58
<b>sNaive (168)</b>	0.57	1.53	1.13	4.84	0.66	1.16	6.62	0.42	0.07	0.55
<b>MLP</b>	0.63	1.49	1.13	1.22	0.32	0.21	5.13	0.4	0.03	0.6
<b>LSTM</b>	0.91	1.90	1.53	1.27	0.43	0.39	3.79	0.61	0.00	0.57
<b>N-BEATS</b>	0.57	1.56	1.12	1.05	0.27	0.20	3.46	0.25	0.02	0.53
<b>TCN</b>	0.43	1.08	0.55	1.5	0.23	0.25	5.45	0.21	0.05	0.59

**Benchmarks** As seen, the forecast error of the sNaive (24) benchmark is not particularly affected by the season of the year as this factor cannot contribute much to the overall accuracy of the method given the short-term (daily) periodicity it assumes. However, sNaive (24) is significantly less accurate on holidays and weekends, which is expected given that said days have different load patterns than weekdays. Mediocre results are also observed for the "time of day" variables as switching among time periods affects the performance of sNaive (24) when transitioning from weekends to weekdays, and vice-versa.

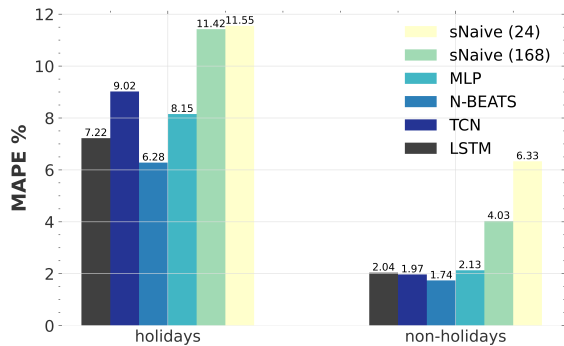
Regarding sNaive (168), the method is less sensitive to the "time of day" features (morning, midday, night) as by using the values of the previous week as forecasts the benchmark manages to capture the weekend to weekday transitions. Similar conclusions are true for the "weekend" variable as well. Nonetheless, on holidays, sNaive (168) still exhibits great errors given that holidays are not subject to weekly seasonality. Additionally, as holidays tend to be concentrated within small periods of time (e.g. Christmas period)—also accompanied by other semi-vacation days due to days off that are given by most companies to their employees—forecasts of weekly seasonality result to low accuracy for long periods of time, both including vacation days and the first week to come after them. With respect to the "season" variables, the forecast error of the sNaive (168) method is negatively affected in winter, which potentially confirms of



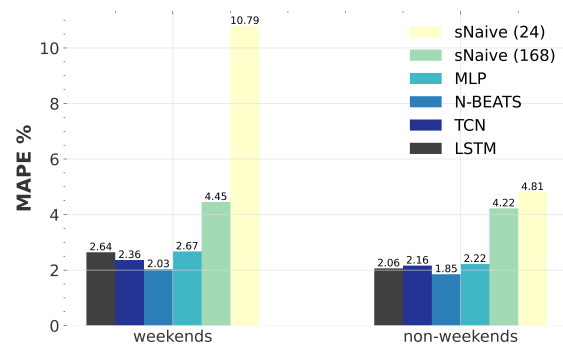
(a) Performance of the models across different times of the day.



(b) Performance of the models across different seasons.



(c) Performance of the models across holidays and non-holiday days.



(d) Performance of the models across weekends and non-weekends.

Figure 4: Performance of the models across different calendar features, as measured by MAPE.

the aforementioned irregularity within the Christmas holidays period. Similarly, “autumn” exhibits a relatively large coefficient value, potentially caused by the switch from summer to autumn that signals the return from holidays and thus an expected notable variation in the load curve from one week to another.

It can be also observed that the increase of the temperature reduces the accuracy of both benchmarks, demonstrating a certain increase in the variability of the time series that cannot be captured effectively by the naive models.

**DL models** Before commenting on the MLR coefficients of the DL models, it should be first noted that all DL architectures perform better on average compared to the naive benchmarks, irrespective of the feature in question. This is expected and confirmed by Figure 4. However, this observation is not to be confused with the MLR coefficient values

as naive models often involve smaller values than DL models, thus denoting a smaller relative increase to their average forecasts error, caused by a specific external variable. Additionally, all advanced DL architectures tend to outperform the MLP apart from some rare cases where LSTM and MLP result to similar error changes.

Regarding the "time of day" variables, MLP, LSTM, and N-BEATS seem to be affected in a similar fashion to sNaive (168), having relatively low coefficient values that indicate a satisfactory modeling of the daily seasonal pattern. Specifically during midday and night, the high variability and the frequent changes in the monotony of the load and the peak load, respectively, lead to greater forecast errors compared to other calendar features, with TCN being however less affected by said changes compared to the rest of the DL models. Concerning midday and night hours, it can be observed that TCN outperforms LSTM and MLP. Yet, even during these periods, TCN cannot surpass N-BEATS in terms of MAPE and RMSE (see Appendix A).

With respect to calendar variables relating to the seasons of the year, the DL models exhibit certain insensitivity to the respective features (winter, spring, autumn). This is confirmed by the relatively small coefficient values alongside Figure 4b where it is found that all DL models produce errors that are relatively close to their average. Note however that during winter months the forecastability of the models decreases significantly compared to other seasons, leading to both increased MLR coefficients and average MAPE values. Among the DL models, N-BEATS and MLP seem to behave better, capturing the patterns of the winter period more successfully.

With regard to holidays, TCN and MLP seem to be more sensitive than sNaive (24) as it can be observed from the larger MLR coefficients of said models. Despite that, all DL models perform better on average than the benchmarks. Nonetheless, "holiday" seems to be the feature that deteriorates most forecast accuracy. This becomes obvious in Figure 1c where a large increase from the average MAPE is observed for all DL models. In this case, LSTM and particularly N-BEATS exhibit the lowest deficits, reaching a MAPE of 7.22 % and 6.28 %, respectively. The relatively small error of the latter model demonstrates the ability of N-BEATS to capture the substantial alterations of the load curve during national holidays, confirming its robustness and superiority throughout distribution shifts that tend to appear less frequently within an electricity load time series.

Concerning the weekend variable, all models—apart from the LSTM— seem to be less sensitive than both naive methods. This may be attributed to the vanishing gradient problem of LSTM networks. Since weekends are observed with a certain periodicity and the input vector of all DL models is larger than a week, weekends are relatively forecastable, resulting to low MLR coefficient values. Again, TCN has the lowest coefficient, N-BEATS demonstrates the best absolute accuracy, while MLP and LSTM reside somewhere in the middle.

Concluding with the temperature variable, all DL models seem to result in more inaccurate forecasts during hotter days. LSTM and N-BEATS seem to be the most insensitive to the changes of temperature, being able to better capture its effect during their learning process irrespective of its purely autoregressive nature. This denotes that architectures that possess memory operations (forget gate of LSTM, backcast of N-BEATS) can better incorporate the effect of weather conditions within their learning procedure.

## 4 Conclusions

This study conducted a comparative analysis of state-of-the-art time series forecasting DL models within the STLTF context, focusing on producing day-ahead forecasts for the Portuguese national net aggregated electricity load. The MLP, LSTM, N-BEATS, and TCN architectures were examined, following a proper hyperparameter tuning and ensembling process.

Our results suggest that ensembling can effectively mitigate the uncertainty of neural weights initialization, resulting to significantly more accurate forecasts than individual models. Moreover, we find that the N-BEATS architecture outperforms the rest of the DL models, reaching a MAPE value of 1.90%, which is 0.32% lower than its competitors. TCN and LSTM perform similar to each other (2.23% and 2.22% respectively), while the MLP follows with a MAPE of 2.34%. Yet, the latter performance is realized with significantly lower computational cost, which may render the utilization of MLPs relevant in certain STLTF applications or for stakeholders that either possess limited computational resources or prefer more energy efficient and sustainable machine learning operations.

In order to investigate the factors that drive the performance of each DL architecture, a MLR model was built per case, correlating the MAPE values of the model with a selected set of calendar and weather features. In this context, national holidays and midday hours proved to be the least forecastable instances overall. TCN was also found to be the most resilient architecture against the fluctuation of external variables, being however consistently outperformed by N-BEATS in absolute error terms.

Regarding future perspectives, this comparative assessment could be replicated using data from more countries, aiming to benchmark the performance of state-of-the-art DL models and investigate the impact of key accuracy drivers more objectively. Additionally, the set of the examined DL architectures could be further expanded to include more models that have been recently proposed in the field. A fully automated MLOps framework is also envisaged, with the objective to enable an automated, off-the-shelf toolkit for model training, validation, evaluation, ensembling and deployment within a context of STLF stakeholders, such as transmission system operators, distribution system operators, aggregators, and energy market operators.

## Acknowledgment

This work has been funded by the European Union’s Horizon 2020 research and innovation programme under the I-ENERGY project, grant agreement No. 101016508. Additionally, the HPC resources utilized for training and optimizing the required machine learning models in this study have been provided by the EGI-ACE project, which also receives funding from the European Union’s Horizon 2020 research and innovation programme under grant agreement No. 101017567.

## References

- [1] Akiba, T., Sano, S., Yanase, T., Ohta, T., Koyama, M., 2019. Optuna: A Next-generation Hyperparameter Optimization Framework, in: Proceedings of the ACM SIGKDD International Conference on Knowledge Discovery and Data Mining, Association for Computing Machinery. pp. 2623–2631. doi:10.1145/3292500.3330701.
- [2] Alla, S., Adari, S.K., 2021. Beginning MLOps with MLFlow. Apress. doi:10.1007/978-1-4842-6549-9.
- [3] Alos, A.L., Bergeron, C., Buontempo, C., Thepaut, J.N., Raoult, B., Biavati, G., Alos, A.L., Bergeron, C., Buontempo, C., Thepaut, J.N., Raoult, B., Biavati, G., 2019. The Copernicus Climate Data Store: ECMWF’s approach to providing online access to climate data and tools. AGUFM 2019, PA31A–05.
- [4] Arvanitidis, A.I., Bargiotas, D., Daskalopulu, A., Laitos, V.M., Tsoukalas, L.H., 2021. Enhanced Short-Term Load Forecasting Using Artificial Neural Networks. Energies 14, 7788. doi:10.3390/en14227788.
- [5] Bahrami, S., Chen, Y.C., Wong, V.W., 2021. Deep Reinforcement Learning for Demand Response in Distribution Networks. IEEE Transactions on Smart Grid 12, 1496–1506. doi:10.1109/TSG.2020.3037066.
- [6] Bai, S., Kolter, J.Z., Koltun, V., 2018. An Empirical Evaluation of Generic Convolutional and Recurrent Networks for Sequence Modeling. arXiv:1803.01271 .
- [7] Bergstra, J., Bardenet, R., Bengio, Y., Kégl, B., 2011. Algorithms for Hyper-Parameter Optimization. Advances in Neural Information Processing Systems 24.
- [8] Chen, L.G., Chiang, H.D., Dong, N., Liu, R.P., 2016. Group-based chaos genetic algorithm and non-linear ensemble of neural networks for short-term load forecasting. IET Generation, Transmission and Distribution 10, 1440–1447. doi:10.1049/iet-gtd.2015.1068.
- [9] Copernicus, EU, 2016. Copernicus land monitoring service. Technical Report.
- [10] Cui, H., Peng, X., 2015. Short-Term City Electric Load Forecasting with Considering Temperature Effects: An Improved ARIMAX Model. Mathematical Problems in Engineering 2015. doi:10.1155/2015/589374.
- [11] De Felice, M., Xin Yao, 2011. Short-Term Load Forecasting with Neural Network Ensembles: A Comparative Study [Application Notes]. IEEE Computational Intelligence Magazine 6, 47–56. doi:10.1109/MCI.2011.941590.
- [12] Farsi, B., Amayri, M., Bouguila, N., Eicker, U., 2021. On short-term load forecasting using machine learning techniques and a novel parallel deep LSTM-CNN approach. IEEE Access 9, 31191–31212. doi:10.1109/ACCESS.2021.3060290.
- [13] Gasparin, A., Lukovic, S., Alippi, C., 2022. Deep learning for time series forecasting: The electric load case. CAAI Transactions on Intelligence Technology 7, 1–25. doi:10.1049/CIT2.12060.
- [14] Grabner, M., Wang, Y., Wen, Q., Blažič, B., Štruc, V., 2022. A Global Modeling Approach for Load Forecasting in Distribution Networks [Preprint]. arXiv:2204.00493 .
- [15] Gu, K., Jia, L., 2020. Temporal Convolutional Network Based Short-term Load Forecasting Model, in: 2020 IEEE 9th Data Driven Control and Learning Systems Conference (DDCLS), IEEE. pp. 584–589. doi:10.1109/DDCLS49620.2020.9275148.

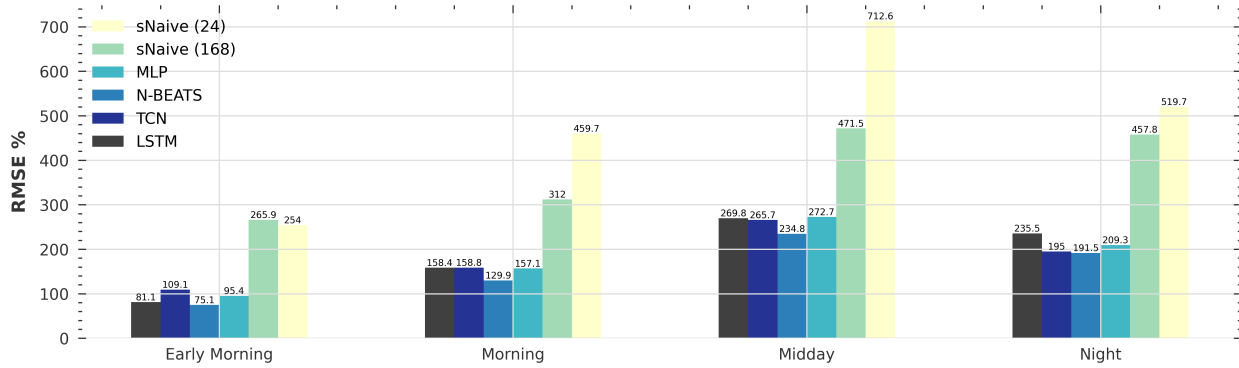


- [16] Haben, S., Giasemidis, G., Ziel, F., Arora, S., 2019. Short term load forecasting and the effect of temperature at the low voltage level. *International Journal of Forecasting* 35, 1469–1484. doi:10.1016/J.IJFORECAST.2018.10.007.
- [17] Hammad, M.A., Jereb, B., Rosi, B., Dragan, D., 2020. Methods and Models for Electric Load Forecasting: A Comprehensive Review. *Logistics & Sustainable Transport* 11, 51–76. doi:10.2478/JLST-2020-0004.
- [18] Henselmeyer, S., Grzegorzec, M., 2021. Short-term load forecasting using an attended sequential encoder-stacked decoder model with online training. *Applied Sciences (Switzerland)* 11. doi:10.3390/app11114927.
- [19] Hernandez, L., Baladron, C., Aguiar, J., Carro, B., Sanchez-Esguevillas, A., Lloret, J., Chinarro, D., Gomez-Sanz, J., Cook, D., 2013. A multi-agent system architecture for smart grid management and forecasting of energy demand in virtual power plants. *IEEE Communications Magazine* 51, 106–113. doi:10.1109/MCOM.2013.6400446.
- [20] Hernandez, L., Baladron, C., Aguiar, J.M., Carro, B., Sanchez-Esguevillas, A.J., Lloret, J., Massana, J., 2014. A survey on electric power demand forecasting: Future trends in smart grids, microgrids and smart buildings. *IEEE Communications Surveys and Tutorials* 16, 1460–1495. doi:10.1109/SURV.2014.032014.00094.
- [21] Hersbach, H., Bell, B., Berrisford, P., Hirahara, S., Horányi, A., Muñoz-Sabater, J., Nicolas, J., Peubey, C., Radu, R., Schepers, D., Simmons, A., Soci, C., Abdalla, S., Abellan, X., Balsamo, G., Bechtold, P., Biavati, G., Bidlot, J., Bonavita, M., De Chiara, G., Dahlgren, P., Dee, D., Diamantakis, M., Dragani, R., Flemming, J., Forbes, R., Fuentes, M., Geer, A., Haimberger, L., Healy, S., Hogan, R.J., Hólm, E., Janisková, M., Keeley, S., Laloyaux, P., Lopez, P., Lupu, C., Radnoti, G., de Rosnay, P., Rozum, I., Vamborg, F., Villaume, S., Thépaut, J.N., 2020. The ERA5 global reanalysis. *Quarterly Journal of the Royal Meteorological Society* 146, 1999–2049. doi:10.1002/QJ.3803.
- [22] Herzen, J., Lässig, F., Piazzetta, S.G., Neuer, T., Tafti, L., Raille, G., Van Pottelbergh, T., Pasięka, M., Skrodzki, A., Huguenin, N., Dumonal, M., Kościsz, J., Bader, D., Gusset, F., Benheddi, M., Williamson, C., Kosinski, M., Petrik, M., Grosch, G., 2021. Darts: User-Friendly Modern Machine Learning for Time Series. *Journal of Machine Learning Research* 23, 1–6. doi:10.48550/arxiv.2110.03224.
- [23] Ho, K., Hsu, Y.Y., Yang, C.C., 1992. Short term load forecasting using a multilayer neural network with an adaptive learning algorithm. *IEEE Transactions on Power Systems* 7, 141–149. doi:10.1109/59.141697.
- [24] Hochreiter, S., Schmidhuber, J., 1997. Long Short-Term Memory. *Neural Computation* doi:10.1162/neco.1997.9.8.1735.
- [25] Huy, P.C., Minh, N.Q., Tien, N.D., Anh, T.T.Q., 2022. Short-Term Electricity Load Forecasting Based on Temporal Fusion Transformer Model. *IEEE Access* 10, 106296–106304. doi:10.1109/ACCESS.2022.3211941.
- [26] Hyndman, R.J., Koehler, A.B., 2006. Another look at measures of forecast accuracy. *International Journal of Forecasting* 22, 679–688. doi:10.1016/j.ijforecast.2006.03.001.
- [27] Kandil, N., Wamkeue, R., Saad, M., Georges, S., 2006. An efficient approach for short term load forecasting using artificial neural networks. *International Journal of Electrical Power & Energy Systems* 28, 525–530. doi:10.1016/j.ijepes.2006.02.014.
- [28] Kang, Y., Hyndman, R.J., Smith-Miles, K., 2017. Visualising forecasting algorithm performance using time series instance spaces. *International Journal of Forecasting* 33, 345–358. doi:10.1016/J.IJFORECAST.2016.09.004.
- [29] Karakolis, E., Pelekis, S., Mouzakitis, S., Markaki, O., Papapostolou, K., Korbakis, G., Psarras, J., 2022. Artificial Intelligence for Next Generation Energy Services Across Europe - The I-ENERGY Project, in: *ES 2021 : 19th International Conference e-Society 2021, Lisbon*. pp. 61–68.
- [30] Koning, A.J., Franses, P.H., Hibon, M., Stekler, H.O., 2005. The M3 competition: Statistical tests of the results. *International Journal of Forecasting* 21, 397–409. doi:10.1016/J.IJFORECAST.2004.10.003.
- [31] Kourentzes, N., Barrow, D.K., Crone, S.F., 2014. Neural network ensemble operators for time series forecasting. *Expert Systems with Applications* 41, 4235–4244. doi:10.1016/J.ESWA.2013.12.011.
- [32] Liao, G.C., Tsao, T.P., 2006. Application of a fuzzy neural network combined with a chaos genetic algorithm and simulated annealing to short-term load forecasting. *IEEE Transactions on Evolutionary Computation* 10, 330–340. doi:10.1109/TEVC.2005.857075.
- [33] Lim, B., Arık, S., Loeff, N., Pfister, T., 2021. Temporal Fusion Transformers for interpretable multi-horizon time series forecasting. *International Journal of Forecasting* 37, 1748–1764. doi:10.1016/J.IJFORECAST.2021.03.012.
- [34] Lin, T., Wang, Y., Liu, X., Qiu, X., 2022. A survey of transformers. *AI Open* 3, 111–132. doi:10.1016/J.AIOPEN.2022.10.001.

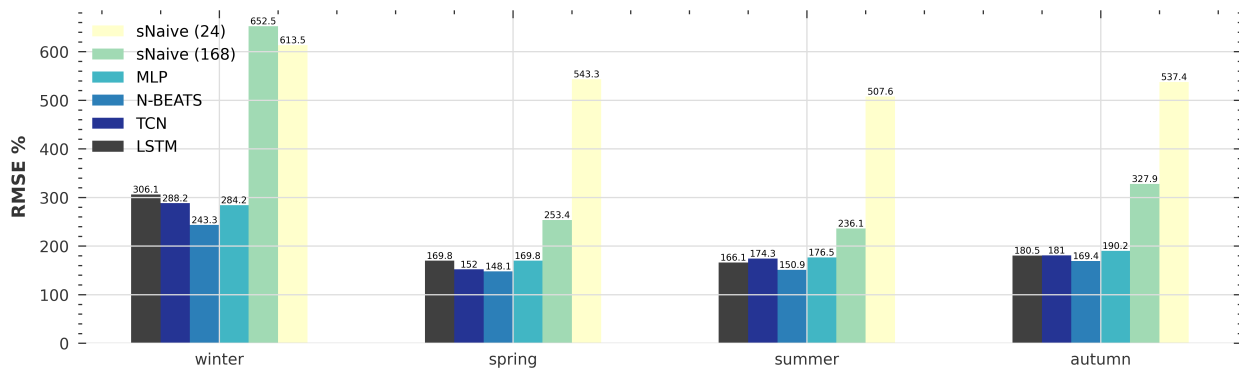
- [35] Mishra, S., Patra, S.K., 2008. Short term load forecasting using neural network trained with genetic algorithm & particle swarm optimization, in: Proceedings - 1st International Conference on Emerging Trends in Engineering and Technology, ICETET 2008, pp. 606–611. doi:10.1109/ICETET.2008.94.
- [36] Moghaddas-Tafreshi, S.M., Farhadi, M., 2008. A linear regression-based study for temperature sensitivity analysis of iran electrical load, in: Proceedings of the IEEE International Conference on Industrial Technology. doi:10.1109/ICIT.2008.4608590.
- [37] Montero-Manso, P., Athanasopoulos, G., Hyndman, R.J., Talagala, T.S., 2020. FFORMA: Feature-based forecast model averaging. *International Journal of Forecasting* 36, 86–92. doi:10.1016/J.IJFORECAST.2019.02.011.
- [38] Moon, J., Rho, S., Baik, S.W., 2022. Toward explainable electrical load forecasting of buildings: A comparative study of tree-based ensemble methods with Shapley values. *Sustainable Energy Technologies and Assessments* 54, 102888. doi:10.1016/J.SETA.2022.102888.
- [39] Oreshkin, B.N., Carpov, D., Chapados, N., Bengio, Y., 2019. N-BEATS: Neural basis expansion analysis for interpretable time series forecasting.
- [40] Oreshkin, B.N., Dudek, G., Peřka, P., Turkina, E., 2021. N-BEATS neural network for mid-term electricity load forecasting. *Applied Energy* 293, 116918. doi:10.1016/J.APENERGY.2021.116918.
- [41] O’Shea, K., Nash, R., 2015. An Introduction to Convolutional Neural Networks. arXiv:1511.08458 .
- [42] Pau, M., Kapsalis, P., Pan, Z., Korbakis, G., Pellegrino, D., Monti, A., 2022. MATRYCS A Big Data Architecture for Advanced Services in the Building Domain. *Energies* 15, 2568. doi:10.3390/EN15072568.
- [43] Pedregosa, F., Michel, V., Grisel, O., Blondel, M., Prettenhofer, P., Weiss, R., Vanderplas, J., Cournapeau, D., Pedregosa, F., Varoquaux, G., Gramfort, A., Thirion, B., Grisel, O., Dubourg, V., Passos, A., Brucher, M., Perrot, M., Duchesnay, E., 2011. Scikit-learn: Machine Learning in Python. *Journal of Machine Learning Research* 12, 2825–2830.
- [44] Pelekis, S., Karakolis, E., Silva, F., Schoinas, V., Mouzakitis, S., Kormpakis, G., Amaro, N., Psarras, J., 2022. In Search of Deep Learning Architectures for Load Forecasting: A Comparative Analysis and the Impact of the Covid-19 Pandemic on Model Performance, in: 2022 13th International Conference on Information, Intelligence, Systems and Applications (IISA), IEEE. pp. 1–8. doi:10.1109/IISA56318.2022.9904363.
- [45] Petropoulos, F., Makridakis, S., Assimakopoulos, V., Nikolopoulos, K., 2014. ‘Horses for Courses’ in demand forecasting. *European Journal of Operational Research* 237, 152–163. doi:10.1016/J.EJOR.2014.02.036.
- [46] Psiloglou, B.E., Giannakopoulos, C., Majithia, S., Petrakis, M., 2009. Factors affecting electricity demand in Athens, Greece and London, UK: A comparative assessment. *Energy* 34, 1855–1863. doi:10.1016/J.ENERGY.2009.07.033.
- [47] Rafi, S.H., Al-Masood, N., Deeba, S.R., Hossain, E., 2021. A short-term load forecasting method using integrated CNN and LSTM network. *IEEE Access* 9, 32436–32448. doi:10.1109/ACCESS.2021.3060654.
- [48] REN, 2022a. REN | Data Hub. URL: <https://datahub.ren.pt/>.
- [49] REN, 2022b. REN | Homepage. URL: <https://www.ren.pt/>.
- [50] Rozemberczki, B., Watson, L., Bayer, P., Yang, H.T., Kiss, O., Nilsson, S., Sarkar, R., 2022. The Shapley Value in Machine Learning. *IJCAI International Joint Conference on Artificial Intelligence* , 5572–5579doi:10.48550/arxiv.2202.05594.
- [51] Rueda, F.D., Suárez, J.D., Torres, A.D.R., 2021. Short-term load forecasting using encoder-decoder wavenet: Application to the french grid. *Energies* 14. doi:10.3390/en14092524.
- [52] Sajjad, M., Khan, Z.A., Ullah, A., Hussain, T., Ullah, W., Lee, M.Y., Baik, S.W., 2020. A Novel CNN-GRU-Based Hybrid Approach for Short-Term Residential Load Forecasting. *IEEE Access* 8, 143759–143768. doi:10.1109/ACCESS.2020.3009537.
- [53] Sehovac, L., Grolinger, K., 2020. Deep Learning for Load Forecasting: Sequence to Sequence Recurrent Neural Networks with Attention. *IEEE Access* 8, 36411–36426. doi:10.1109/ACCESS.2020.2975738.
- [54] Singh, N.P., Joshi, A.R., Alam, M.N., 2022. Short-Term Forecasting in Smart Electric Grid Using N-BEATS. *ICPC2T 2022 - 2nd International Conference on Power, Control and Computing Technologies, Proceedings* doi:10.1109/ICPC2T53885.2022.9776757.
- [55] Spiliotis, E., Doukas, H., Assimakopoulos, V., Petropoulos, F., 2021. Forecasting week-ahead hourly electricity prices in Belgium with statistical and machine learning methods. *Mathematical Modelling of Contemporary Electricity Markets* , 59–74doi:10.1016/B978-0-12-821838-9.00005-0.

- [56] Spiliotis, E., Kouloumos, A., Assimakopoulos, V., Makridakis, S., 2020. Are forecasting competitions data representative of the reality? *International Journal of Forecasting* 36, 37–53. doi:10.1016/J.IJFORECAST.2018.12.007.
- [57] Steffen, B., Patt, A., 2022. A historical turning point? Early evidence on how the Russia-Ukraine war changes public support for clean energy policies. *Energy Research & Social Science* 91, 102758. doi:10.1016/J.ERSS.2022.102758.
- [58] Talagala, T.S., Li, F., Kang, Y., 2022. FFORMPP: Feature-based forecast model performance prediction. *International Journal of Forecasting* 38, 920–943. doi:10.1016/J.IJFORECAST.2021.07.002.
- [59] Tang, X., Chen, H., Xiang, W., Yang, J., Zou, M., 2022. Short-Term Load Forecasting Using Channel and Temporal Attention Based Temporal Convolutional Network. *Electric Power Systems Research* 205, 107761. doi:10.1016/J.EPSR.2021.107761.
- [60] UCI, 2022. UCI Machine Learning Repository | ElectricityLoadDiagrams20112014 Data Set. URL: <https://archive.ics.uci.edu/ml/datasets/ElectricityLoadDiagrams20112014>.
- [61] Vesa, A., Cioara, T., Anghel, I., Antal, M., Pop, C., Sustainability, B.I., 2020, U., 2020. Energy flexibility prediction for data center engagement in demand response programs. *MDPI* 12, 1417. doi:<https://doi.org/10.3390/su12041417>.
- [62] Wehrmeister, K.A., Bothos, E., Marinakis, V., Magoutas, B., Pastor, A., Carreras, L., Monti, A., 2022. The BD4NRG Reference Architecture for Big Data Driven Energy Applications. 13th International Conference on Information, Intelligence, Systems and Applications, IISA 2022 doi:10.1109/IISA56318.2022.9904424.
- [63] Wen, H., Gu, J., Ma, J., Yuan, L., Jin, Z., 2021. Probabilistic Load Forecasting via Neural Basis Expansion Model Based Prediction Intervals. *IEEE Transactions on Smart Grid* 12, 3648–3660. doi:10.1109/TSG.2021.3066567.
- [64] Wu, K., Gu, J., Meng, L., Wen, H., Ma, J., 2022. An explainable framework for load forecasting of a regional integrated energy system based on coupled features and multi-task learning. *Protection and Control of Modern Power Systems* 7, 1–14. doi:10.1186/S41601-022-00245-Y/TABLES/7.
- [65] Yin, L., Xie, J., 2021. Multi-temporal-spatial-scale temporal convolution network for short-term load forecasting of power systems. *Applied Energy* 283, 116328. doi:10.1016/J.APENERGY.2020.116328.
- [66] Zhang, G., Wei, C., Jing, C., Wang, Y., 2022. Short-Term Electrical Load Forecasting Based on Time Augmented Transformer. *International Journal of Computational Intelligence Systems* 15, 1–11. doi:10.1007/S44196-022-00128-Y/FIGURES/6.
- [67] Zhang, R., Dong, Z.Y., Xu, Y., Meng, K., Wong, K.P., 2013. Short-term load forecasting of Australian national electricity market by an ensemble model of extreme learning machine. *IET Generation, Transmission and Distribution* 7, 391–397. doi:10.1049/iet-gtd.2012.0541.

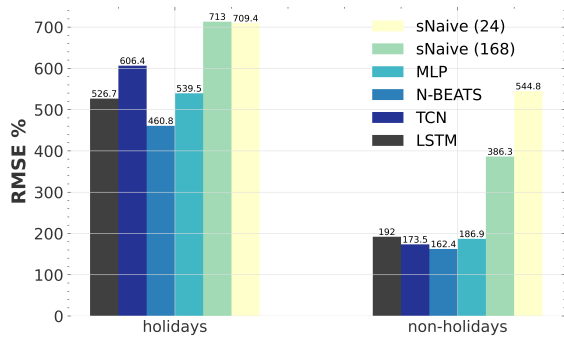
## A Figures



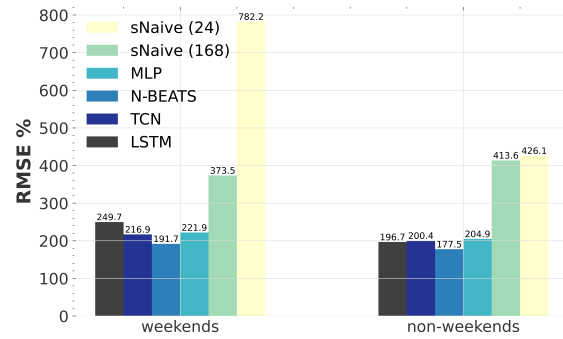
(a) Performance of the models across the times of day



(b) Performance of the models across seasons



(c) Performance of the models across holidays and non-holidays



(d) Performance of the models across weekends and non-weekends

Figure A.1: Performance of the models across external variables measured by the RMSE evaluation metric